

Detection of Osteoporosis Using Knee X-Rays

Sanika M. Rangayyan

*PES Center for Pattern Recognition
Dept. of CSE, PES University
Bengaluru, India
sanrangayyan@gmail.com*

Divya K.

*PES Center for Pattern Recognition
Dept. of CSE, PES University
Bengaluru, India
divya110702@gmail.com*

Ishaan Shettigar

*PES Center for Pattern Recognition
Dept. of CSE, PES University
Bengaluru, India
ishaanshettigar@gmail.com*

Jimish Mrug

*PES Center for Pattern Recognition
Dept. of CSE, PES University
Bengaluru, India
mrugjimish@gmail.com*

Rajesh R.

*Dept. of Radiology
Mandya Institute of Medical Sciences
Mandya, India
rajeshiyer81@gmail.com*

Gowri Srinivasa

*PES Center for Pattern Recognition
Dept. of CSE, PES University
Bengaluru, India
gsrinivasa@pes.edu*

Abstract—This study presents a pipeline for the automated detection of osteoporosis in knees using X-ray images. In particular, we identified trabecular patterns, that serve as an important indicator of osteoporosis, in the images of affected subjects. In addition to incorporating image features for trabecular patterns, we examined the efficacy of a multimodal approach that incorporates auxiliary patient details: subject age and gender, which have been reported to be good indicators of osteoporosis. The results are promising and demonstrate the potential of the proposed solution approach to provide an accessible and inexpensive assessment option for osteoporosis.

Index Terms—knee X-ray, multimodal analysis, trabecular patterns

I. INTRODUCTION

Osteoporosis is a bone condition that weakens and makes bones fragile, increasing the risk of fracture [1]. With more than 200 million cases worldwide [2], osteoporosis is a common medical problem, particularly in elderly people [3] and postmenopausal women [4]. Osteoporosis, initially asymptomatic [5], progresses to cause fractures and back pain [6] and is the cause of fracture in more than 8.9 million people worldwide annually [7]. Early identification allows for proactive treatments such as bisphosphonates, teriparatides [8], supplements [9], exercise, and fall prevention.

The WHO designates dual-energy X-ray absorptiometry (DXA) as the gold standard for diagnosing osteoporosis [10] [11]. Bone mineral density (BMD), measured in g/cm^2 , is the ratio of bone mineral content (BMC) to the tested bone area [12]. BMD values, often reported as standard deviation units (SD) or T-scores, use the latter to measure deviations below the mean BMD for healthy young individuals. A T-score of 1.0 or more is normal, and - 2.5 or less is osteoporosis [13]. Despite its accuracy, DEXA's limited availability in rural areas poses a challenge [14]. In contrast, X-ray technology, widely used in healthcare settings, is practical, accessible, and cost-

effective for routine osteoporosis screening [15].

Age and gender both contribute significantly to osteoporosis. Compared with men, women typically experience the onset of bone loss earlier. Both men and women lose bone density, although women tend to do so at a faster rate, at a younger age, and with higher levels of markers associated with bone resorption [16]. Men are also affected by age-related bone loss, which is characterized by slow and progressive deterioration. Osteoporosis is often associated with the deterioration of bone composition, structure, and function that occurs with age [17]. Hence, age and gender must be considered together to obtain a better understanding of the prevalence of osteoporosis.

To address the foregoing challenges, this work proposes automating the detection of osteoporosis using knee X-rays. The project aims to leverage machine learning algorithms and image processing techniques to develop a model that can efficiently detect abnormalities in the knee using image data, patient data, and a multimodal approach. In addition, the project detects the presence of trabecular patterns, which is a major indicator of osteoporosis [18].

The key contributions of the study include (i) evaluating the utility of incorporating patient data, such as age and gender, along with image data in the decision-making, (ii) use of image processing techniques to enhance the trabecular patterns, if present, in the images and (iii) an analysis of intensity that makes the model's decision reliable. Further, this study uses the largest indigenous X-ray data concerning screening for osteoporosis.

II. RELATED WORK

The advent of deep learning architectures holds much promise for the detection of regions of interest, such as trabecular patterns, in X-ray images. However, the small sample sizes are more amenable to transfer learning. One of the earlier works in this direction compared the performances of four well-known architectures: AlexNet, VGG16, ResNet18, and

VGG19 to classify an X-ray image as ‘normal’ or ‘osteoporotic’ [19] using open-source Mendeley data for the study. Despite promising results, the authors mention the low volume of data available as a limitation of this approach.

In the study [20], VGG16 with and without fine-tuning were the two CNN models employed on the Mendeley data. It was observed that, compared with the model without fine-tuning, the VGG16 with fine-tuning provided greater accuracy. This study also faced the constraint of the low volume of data.

The dataset used in the study [21] is an amalgamation of two different datasets: a research dataset and a public data set from Kaggle. It study proposed Osteo-Net, a deep learning architecture for knee X-ray image-based osteoporosis diagnosis. Using the gradient-weighted class activation mapping (Grad-CAM) technique, the regions most important for the expected probability of an image belonging to a predefined class were highlighted. This study utilized only the image data for detecting osteoporosis in the knees.

An ensemble deep learning model was used by the authors in [22] for detecting osteoporosis in dental radiographs that used image data and clinical data. ResNet18, 152 and EfficientNet b0, b3, b7 were used along with focused visualization using guided Grad-CAM. The study showed that having an ensemble model produced better results than a normal CNN model.

The Single index is the most widely used method for examining how the proximal femur’s structure changes with age. However, the subjectivity involved in determining grades can limit its practical value. To describe the trabecular pattern changes in the proximal femur that are seen on radiographs and contribute to the assessment of osteoporosis, the research [23] used several texture analysis approaches. 41 radiographs were ranked using texture analysis and then compared to the Single index grading carried out by knowledgeable specialists. To extract the characteristics that describe the structural change in trabecular patterns, the authors examined three texture analysis methods: wavelet transformations, fractal dimension, and the Gabor filter. One method for evaluating osteoporosis is to examine the trabecular patterns.

The purpose of this study [24] was to determine whether the morphological features of the trabecular bones in the maxilla and mandible changed between patients with osteoporosis and normal controls. Peripheral radiographs from the dentists of 12 control subjects and 11 patients with osteoporosis were collected. A computer program measured the trabecular architecture’s morphological characteristics. This information was consistent with the theory that, when compared with normal people, patients with osteoporosis exhibit a different trabecular pattern in their jaws.

III. DATASET

Data has been obtained from the Mandya Institute of Medical Sciences (MIMS), an independent government medical school governed by the Government of Karnataka in accordance with the Declaration of Helsinki. The study has not influenced either the diagnosis or treatment of any of the subjects and the present study to develop a computational model to aid in the detection of osteoporosis has been entirely retrospective. We have meticulously collected data from outpatient discharges. One-third of the outpatient discharges came from the radiology department, which provided large and comprehensive data. The data was collected in DICOM (Digital Imaging and Communications in Medicine) format with the help of the patient ID. The corresponding age and gender of the patients were stored in a CSV file. The DICOM images are of dimension and 1678×2307 , and a bit depth of 12. A standard window length of 2048 and a window width of 4096 were maintained throughout the dataset during collection.

The team collected nearly 700 knee X-ray images, which were classified as normal, abnormal, and mildly abnormal. Abnormality may include the conditions of osteoporosis and osteoarthritis, as these are the two major disorders of the bones. Since the screening pertained to subjects who had some reason to undergo the imaging test, 500 images exhibited some abnormality. The ground truth was obtained from the manual annotation of the images by clinical practitioners. There are roughly, 200 osteoporosis images (that also exhibited signs of osteoarthritis), 200 images with a mild abnormality (either osteoporosis or osteoarthritis or both), and 300 images that were ‘normal’ (i.e., not diagnosed with either osteoporosis or osteoarthritis). In the present study, we focus on the detection of (any trace of) osteoporosis only. Sample images from the dataset are shown in Fig. 1.



Fig. 1: Sample images of a normal knee, a mildly abnormal knee, and a knee showing severe abnormalities.

IV. METHODOLOGY

Our methodology encompasses machine learning algorithms and image processing techniques in a unique pipeline (see Fig. 2). We adopted an early fusion strategy to incorporate age and gender along with the X-ray images. In addition, trabecular patterns, which are the major indicator of osteoporosis, are highlighted using image processing providing better visual evidence.

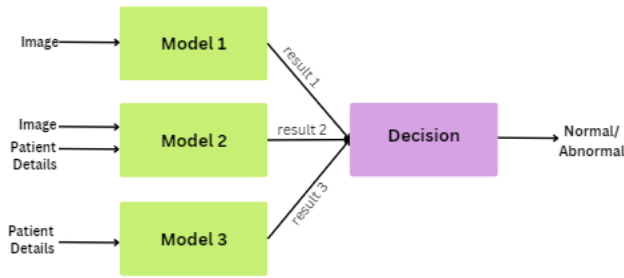


Fig. 2: Schematic diagram of the pipeline to screen for osteoporosis using X-ray images.

A. Comparison of the outcomes of a multimodal analysis involving both images and patient details, and classification models that utilized only images and patient details.

This study incorporates a multimodal approach to classify knee images. We investigated three different models in this study: one based only on knee images, one using patient demographics (age and gender) only, and a third using an early fusion strategy to combine image and patient detail data. Predicting whether the knee image is abnormal or normal is the main objective.

The YOLOv8 object detection model was used for region-of-interest (ROI) detection to crop the images to focus only on the knee region. 380 images were manually annotated, with a focus on the femur, joint, and tibia regions. A YOLOv8-medium object detection model was used from Ultralytics for training, with the image size set to 1024 and the batch size set to 4. In the tabular data, the gender column consisted of values (M, F) that were binarized, the age column consisted of values from 20 to 80 that were scaled using Minmax scaling, and the diagnosis column consisted of values (N, A) that were binarized.

1) Image-based model

Two different models were used, one with and one without fine-tuning. By adjusting the last fully connected layer of a pre-trained ResNet18 model, fine-tuning allows it to adapt to the particular task of knee image classification. For data augmentation, random horizontal flips were applied to the training set. The mean and standard deviation of the images were calculated across the data set, and the images were normalized. Both the training and validation sets underwent image transformations, such as resizing to a fixed size of (224, 224) and conversion to PyTorch tensors. In the training loop, cross-entropy loss serves as the optimization criterion, and stochastic gradient descent (SGD) is the optimizer. The implementation of learning rate scheduling used a decay factor of 0.1 every seven epochs. The validation and training sets were used for model evaluation. The performance of the model was graphically assessed using the predicted and ground truth labels. To visualize the performance, a graph was plotted be-

tween the test and train accuracies and the test and train losses. In addition, a confusion matrix was computed and printed. On the given data, various models such as EfficientNet and DenseNet were performed, among which ResNet18 produced the highest accuracy.

2) Patient details-based model

An Excel file containing patient information after preprocessing the independent and target variables was loaded into Pandas DataFrame. Rows with NULL values were eliminated from the data frame. The dataset was split into features such as age and gender, and the target variable was diagnosis. To balance the classes, oversampling using the Synthetic Minority Over-sampling Technique (SMOTE) was used. To preserve the proportion of classes in each fold, the dataset was divided into k folds. Predictions were made on the test fold after the classification model was trained on the training folds for each fold. A thorough classification report was printed, which included a summary of the support, recall, F1-score, and precision of the two classes. The accuracy list's mean and standard deviation were computed and reported over a 10-fold cross-validation. Of the models, logistic regression produced the most accurate results.

3) Multimodal model

A ResNet18 architecture was employed as the backbone for image feature extraction. To obtain a feature representation, the final two layers of ResNet18 were eliminated. The model was pre-trained to extract hierarchical features from the knee images. A function was written to retrieve ResNet18 features from knee images. Image preprocessing included resizing, normalization, and tensor conversion. Features were obtained by forwarding the preprocessed image through the modified ResNet18 model (see Fig. 3). Features were flattened to form a comprehensive representation of each image. Patient data from the preprocessed CSV file were concatenated with ResNet18 features. A split of 80:20 was used to divide the dataset into testing and training sets. Models such as XGBoost and SVM (sigmoid, rbf, and poly kernel) were trained. Once the classification model has been trained on the training folds for each fold, predictions are made on the test fold. Accuracy and a classification report were generated for each fold. After a 10-fold cross-validation, the mean and standard deviation of the accuracy list were computed and displayed.

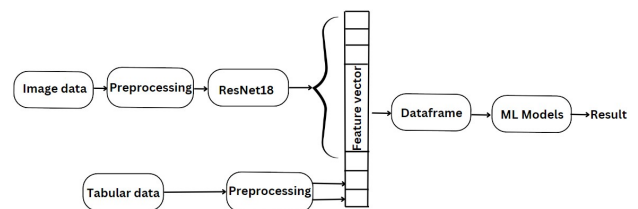


Fig. 3: Architecture for multimodal model classification of the presence of any abnormality in knee X-ray images and patient data.

This multimodal approach improves knee pathology classification by combining information-based on patient details and images.

B. Visually interpretable technique for analyzing trabecular patterns

The previous section explained the architecture, which considers both image data and patient details. Classification models predict whether the knee is normal or abnormal. Abnormal knees are either osteoporotic or osteoarthritic. This section includes the detection of trabecular patterns in the knee to indicate osteoporosis.

1) Detection of trabecular patterns

A clear indicator of the underlying bone loss in osteoporotic knees is the highlighted trabecular pattern. Radiologists can determine the severity of osteoporosis by analyzing how trabecular patterns appear on X-rays. Making treatment decisions and diagnosing osteoporosis heavily depend on this information. These patterns can be highlighted using various methods. One such method used in this research is an edge detection algorithm in MATLAB. The code takes the folder containing DICOM files and loops through each file using the command 'dicomread'. DICOM images are normalized by dividing them by the maximum pixel. The Sobel filter is convolved on the image to detect the vertical edges. This was done using 'imfilter' and 'fspecial'. A Sobel response above a threshold will determine whether to create a binary image ('horizontal edges'). Different threshold values were experimented with to match the ground truth label. The appropriate threshold obtained was 0.15. Morphological operations were used to eliminate the binary image's minuscule edges. When a connected component (small edge) had fewer pixels than the given 'minEdgeLength', 'bwareaopen' eliminated it. Again, different threshold values were experimented with to match the ground truth label of whether the knee image being used has prominent trabecular patterns or not. The approximate threshold obtained was 50. The output image was visualized.

There are cases where the knee can have both osteoporosis and osteoarthritis. The above methods made the detection of osteoporosis more explainable.

V. RESULTS AND DISCUSSION

Table I summarises the accuracy results obtained by training an image-based model, a patient-details-based model, and a multimodal model.

A. Image-based model for abnormality detection

We observe that the ResNet18 model with fine-tuning produces the highest accuracy compared to ResNet18 without fine-tuning and outperforms the other models that were tested as well.

In the fine-tuned ResNet18 model, we observe that the validation loss decreases with the epochs (see Fig. 5) and the validation accuracy increases. The model was tested on 40

TABLE I: Detection of osteoporosis

Purpose	Model	Accuracy
Image-based abnormality detection	ResNet18 without fine-tuning	85.96%
Image-based abnormality detection	ResNet18 with fine-tuning	89.47%
Patient data-based abnormality detection	Logistic regression	84 \pm 0.062%
Multimodal-based abnormality detection	XGBoost	86.61 \pm 0.065%

images to obtain the confusion matrix and the graph (see Fig. 4). The presence of high-quality medical images aided in achieving better accuracy.

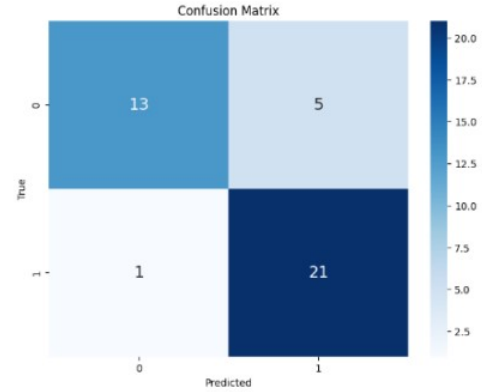


Fig. 4: Confusion matrix of image-based model

B. Patient details-based model for abnormality detection

The use of only patient details such as age and gender is believed to be correlated with degenerative osteo disorders, but may not produce as good an interpretation as the image data. However, it can be used to get a better understanding of the risk of developing the disorder over time across the two genders. The logistic regression model produced the highest accuracy compared with models such as Random Forest, XGBoost, and SVM (see Fig. 6).

C. Multimodal model for abnormality detection

The aim was to observe whether the patient data boosted accuracy if concatenated with image data. For this comparison, an early fusion approach was used with ResNet18 as a feature extractor, which was compared with ResNet18 for image-only classification. Early fusion of age and gender with image features resulted in a slight increase in accuracy. Fig. 7 presents the confusion matrix obtained on the testing data.

D. Detection of trabecular patterns

Using image processing technique, we were able to enhance the vertical trabecular patterns in the knee X-ray image. This method was approved by the radiologist. By highlighting subtle patterns and changes that may be difficult to discern with the naked eye, this technology may assist doctors in

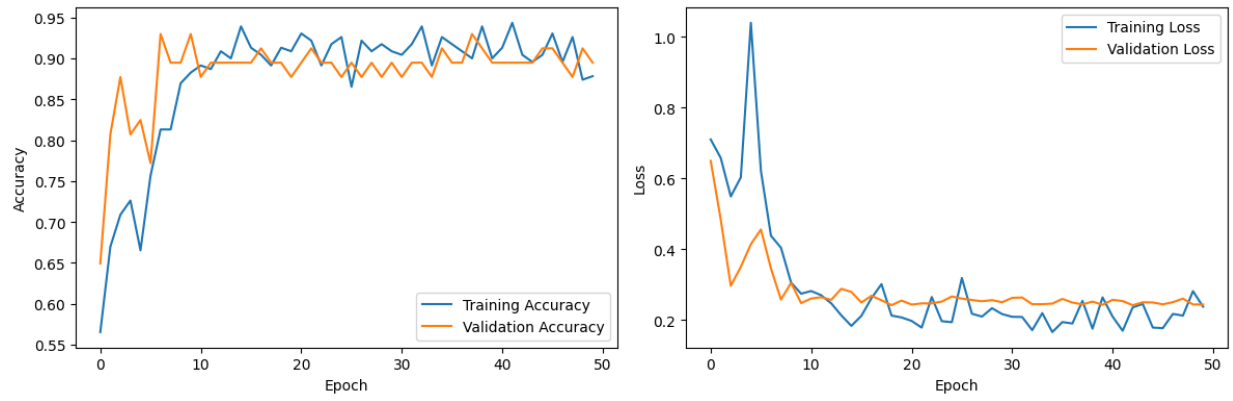


Fig. 5: Training and validation graphs of image-based model

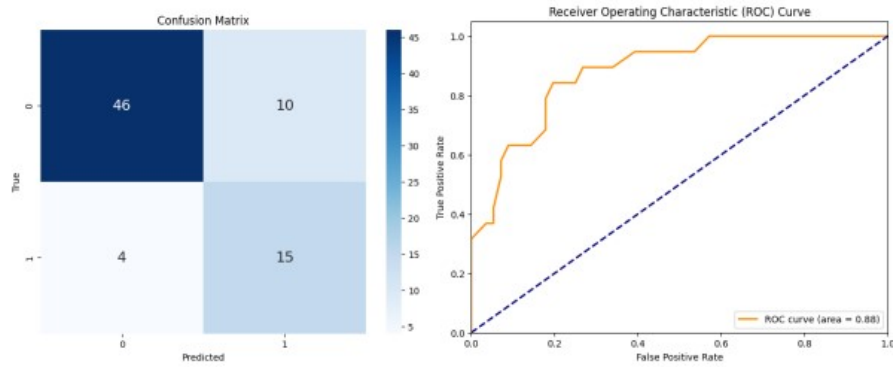


Fig. 6: Confusion matrix and ROC curve for the patient details-based model.

diagnosing osteoarthritis more accurately and efficiently. We observe that the knees in Fig. 8 and Fig. 9 are osteoporotic, as we observe that the trabecular patterns are highlighted in the corresponding image, whereas the knee in Fig. 10 is normal.

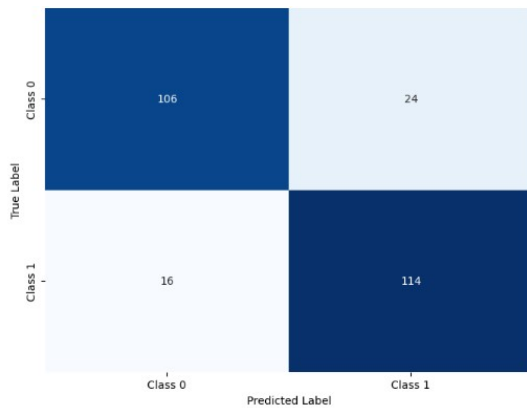


Fig. 7: Confusion matrix of multimodal model



Fig. 8: Original image and image with enhanced trabecular patterns.

VI. CONCLUSION

The goal of this study was to address the challenge of detecting osteoporosis, a common musculoskeletal disorder. As the chances of knees being osteoporotic are high in postmenopausal and elderly people, adding a factor of gender and age boosted the accuracy of the model. The output of the image processing, resulting in an edge map, aids in better visualization of the presence of osteoporosis by observing the intensity of the trabecular patterns highlighted in the edge map. The study can be extended to investigate severity as

a classification factor. The current study did not specifically address the degree or severity of osteoporosis or osteoarthritis; rather, it concentrated on determining their presence.



Fig. 9: Original image and image with enhanced trabecular patterns.



Fig. 10: Original image and image without trabecular patterns.

REFERENCES

- [1] T. Coughlan and F. Dockery, "Osteoporosis and fracture risk in older people," *Clinical medicine*, vol. 14, no. 2, p. 187, 2014.
- [2] T. Sözen, L. Özişik, and N. Ç. Başaran, "An overview and management of osteoporosis," *European journal of rheumatology*, vol. 4, no. 1, p. 46, 2017.
- [3] N. Salari, H. Ghasemi, L. Mohammadi, M. H. Behzadi, E. Rabieenia, S. Shohaimi, and M. Mohammadi, "The global prevalence of osteoporosis in the world: a comprehensive systematic review and meta-analysis," *Journal of orthopaedic surgery and research*, vol. 16, pp. 1–20, 2021.
- [4] R. Sander, "Asymptomatic osteoporosis masks the importance of taking medication," *Nursing Older People*, vol. 19, no. 10, pp. 23–23, 2007.
- [5] R. Khinda, S. Valecha, N. Kumar, J. Walia, K. Singh, S. Sethi, A. Singh, M. Singh, P. Singh, and S. Mastana, "Prevalence and predictors of osteoporosis and osteopenia in postmenopausal women of punjab, india," *International Journal of Environmental Research and Public Health*, vol. 19, no. 5, p. 2999, 2022.
- [6] A. Sarmast, A. Kirmani, and A. Bhat, "Osteoporosis presenting as low backache: an entity not uncommon to be missed," *Asian Journal of Neurosurgery*, vol. 13, no. 03, pp. 693–696, 2018.
- [7] F. Pouresmaeili, B. Kamalidehghan, M. Kamarehei, and Y. M. Goh, "A comprehensive overview on osteoporosis and its risk factors," *Therapeutics and clinical risk management*, pp. 2029–2049, 2018.
- [8] G. Fan, Q. Zhao, P. Lu, H. Chen, W. Tan, W. Guo, C. Liu, and J. Liu, "Comparison between teriparatide and bisphosphonates for improving bone mineral density in postmenopausal osteoporosis patients: A meta-analysis," *Medicine*, vol. 99, no. 15, 2020.
- [9] J. A. Sunyecz, "The use of calcium and vitamin d in the management of osteoporosis," *Therapeutics and clinical risk management*, vol. 4, no. 4, pp. 827–836, 2008.
- [10] G. M. Blake and I. Fogelman, "The role of dxa bone density scans in the diagnosis and treatment of osteoporosis," *Postgraduate medical journal*, vol. 83, no. 982, pp. 509–517, 2007.
- [11] M. Punda and S. Grazio, "Bone densitometry—the gold standard for diagnosis of osteoporosis," *Reumatizam*, vol. 61, no. 2, pp. 70–74, 2014.
- [12] J. A. Kanis, E. V. McCloskey, H. Johansson, A. Oden, L. J. Melton III, and N. Khaltayev, "A reference standard for the description of osteoporosis," *Bone*, vol. 42, no. 3, pp. 467–475, 2008.
- [13] E. Siris, R. Adler, J. Bilezikian, M. Bolognese, B. Dawson-Hughes, M. Favus, S. Harris, S. Jan de Beur, S. Khosla, N. Lane *et al.*, "The clinical diagnosis of osteoporosis: a position statement from the national bone health alliance working group," *Osteoporosis international*, vol. 25, pp. 1439–1443, 2014.
- [14] K. E. Cherian, N. Kapoor, M. Meeta, and T. V. Paul, "Screening tools for osteoporosis in india: Where do we place them in current clinical care?" *Journal of Mid-life Health*, vol. 12, no. 4, p. 257, 2021.
- [15] D. S.-R. Maru, R. Schwarz, J. Andrews, S. Basu, A. Sharma, and C. Moore, "Turning a blind eye: the mobilization of radiology services in resource-poor regions," *Globalization and health*, vol. 6, no. 1, pp. 1–8, 2010.
- [16] K. A. Alswat, "Gender disparities in osteoporosis," *Journal of clinical medicine research*, vol. 9, no. 5, p. 382, 2017.
- [17] O. Demontiero, C. Vidal, and G. Duque, "Aging and bone loss: new insights for the clinician," *Therapeutic advances in musculoskeletal disease*, vol. 4, no. 2, pp. 61–76, 2012.
- [18] M. Morita, A. Ebihara, M. Itoman, and T. Sasada, "Progression of osteoporosis in cancellous bone depending on trabecular structure," *Annals of biomedical engineering*, vol. 22, pp. 532–539, 1994.
- [19] I. M. Wani and S. Arora, "Osteoporosis diagnosis in knee x-rays by transfer learning based on convolution neural network," *Multimedia Tools and Applications*, vol. 82, no. 9, pp. 14 193–14 217, 2023.
- [20] U. B. Abubakar, M. M. Boukar, and S. Adeshina, "Evaluation of parameter fine-tuning with transfer learning for osteoporosis classification in knee radiograph," *International Journal of Advanced Computer Science and Applications*, vol. 13, no. 8, 2022.
- [21] A. Kumar, R. C. Joshi, M. K. Dutta, R. Burget, and V. Myska, "Osteonet: A robust deep learning-based diagnosis of osteoporosis using x-ray images," in *2022 45th International Conference on Telecommunications and Signal Processing (TSP)*. IEEE, 2022, pp. 91–95.
- [22] S. Sukegawa, A. Fujimura, A. Taguchi, N. Yamamoto, A. Kitamura, R. Goto, K. Nakano, K. Takabatake, H. Kawai, H. Nagatsuka *et al.*, "Identification of osteoporosis using ensemble deep learning model with panoramic radiographs and clinical covariates," *Scientific reports*, vol. 12, no. 1, p. 6088, 2022.
- [23] N. Bayramoglu, A. Tiulpin, J. Hirvasniemi, M. T. Nieminen, and S. Saarakkala, "Adaptive segmentation of knee radiographs for selecting the optimal roi in texture analysis," *Osteoarthritis and Cartilage*, vol. 28, no. 7, pp. 941–952, 2020.
- [24] S. C. White and D. J. Rudolph, "Alterations of the trabecular pattern of the jaws in patients with osteoporosis," *Oral Surgery, Oral Medicine, Oral Pathology, Oral Radiology, and Endodontology*, vol. 88, no. 5, pp. 628–635, 1999.